UC Irvine
UC Irvine Previously Published Works

Title

Attribution of projected changes in summertime US ozone and $PM_{2.5}$ concentrations to global changes

Permalink

https://escholarship.org/uc/item/2kq7z7m5

Journal

Atmospheric Chemistry and Physics, 9(4)

ISSN

1680-7316

Authors

Avise, J
Chen, J
Lamb, B
et al.

Publication Date

2009

DOI

10.5194/acp-9-1111-2009

Copyright Information

Peer reviewed

**Atmospheric
Chemistry
and Physics**

Attribution of projected changes in summertime US ozone and PM$_{2.5}$ concentrations to global changes

J. Avise[1,*], **J. Chen**[1,**], **B. Lamb**[1], **C. Wiedinmyer**[2], **A. Guenther**[2], **E. Salathé**[3], **and C. Mass**[3]

[1]Laboratory for Atmospheric Research, Washington State University, Pullman, Washington, USA
[2]National Center for Atmospheric Research, Boulder, Colorado, USA
[3]University of Washington, Seattle, Washington, USA
[*]now at: California Air Resources Board, Sacramento, CA, USA
[**]now at: National Research Council of Canada, Ottawa, ON, Canada

Abstract. The impact that changes in future climate, anthropogenic US emissions, background tropospheric composition, and land-use have on summertime regional US ozone and PM$_{2.5}$ concentrations is examined through a matrix of downscaled regional air quality simulations, where each set of simulations was conducted for five months of July climatology, using the Community Multi-scale Air Quality (CMAQ) model. Projected regional scale changes in meteorology due to climate change under the Intergovernmental Panel on Climate Change (IPCC) A2 scenario are derived through the downscaling of Parallel Climate Model (PCM) output with the MM5 meteorological model. Future chemical boundary conditions are obtained through downscaling of MOZART-2 (Model for Ozone and Related Chemical Tracers, version 2.4) global chemical model simulations based on the IPCC Special Report on Emissions Scenarios (SRES) A2 emissions scenario. Projected changes in US anthropogenic emissions are estimated using the EPA Economic Growth Analysis System (EGAS), and changes in land-use are projected using data from the Community Land Model (CLM) and the Spatially Explicit Regional Growth Model (SERGOM). For July conditions, changes in chemical boundary conditions are found to have the largest impact (+5 ppbv) on average daily maximum 8-h (DM8H) ozone. Changes in US anthropogenic emissions are projected to increase average DM8H ozone by +3 ppbv. Land-use changes are projected to have a significant influence on regional air quality due to the impact these changes have on biogenic hydrocarbon emissions. When climate changes and land-use changes are considered simultaneously, the average DM8H ozone decreases due to a reduction in biogenic VOC emissions (−2.6 ppbv). Changes in average 24-h (A24-h) PM$_{2.5}$ concentrations are dominated by projected changes in anthropogenic emissions (+3 μg m^{-3}), while changes in chemical boundary conditions have a negligible effect. On average, climate change reduces A24-h PM$_{2.5}$ concentrations by −0.9 μg m^{-3}, but this reduction is more than tripled in the Southeastern US due to increased precipitation and wet deposition.

1 Introduction

Reduced air quality due to increased levels of ozone and PM$_{2.5}$ is the result of a complex mix of chemical reactions and physical processes in the atmosphere. These reactions and processes are predominantly influenced by pollutant emissions and meteorological conditions. Consequently, global changes in climate and trace gas emissions from both anthropogenic and biogenic sources may have a profound impact on future air quality. In particular, global climate change can directly affect air quality through changes in regional temperatures, which will influence chemical reaction rates in the atmosphere (Sillman and Samson, 1995). The work of Dawson et al. (2007) found that during a July ozone episode over the Eastern US, temperature was the meteorological parameter that had the greatest influence on 8-h ozone concentrations, with an average increase in 8-h ozone of 0.34 ppb/°K. In addition to temperature, global climate changes may directly impact other boundary layer parameters that are important to regional air quality, such as boundary layer height, cloud formation, and the occurrence of

stagnation events. Leung and Gustafson Jr. (2005) investigated the potential effects of climate change on US air quality, and found that changes in temperature, downward solar radiation, rainfall frequency, and the frequency of stagnation events were likely to impact regional air quality in the future. The work of Mickley et al. (2004) also examined the impact of climate change on regional air quality in the US, and found that summertime air quality in the Midwestern and Northeastern US was projected to worsen due to a decrease in the frequency of mid-latitude cyclones across Southern Canada.

Changes in anthropogenic and biogenic emissions may also have a substantial influence on future air quality. Changes in anthropogenic emissions (excluding control-related reductions) are primarily driven by population growth and urbanization. The IPCC (Intergovernmental Panel on Climate Change) estimates the global population will grow from 5.3 billion in 1990 to between 8.7 and −1.3 billion by the year 2050 (Nakićenović et al., 2000). The IPCC SRES (Special Report on Emission Scenarios) projects that over the next 50 years global emissions of the ozone precursors NO_x ($NO+NO_2$) and non-methane volatile organic compounds (NMVOCs) may increase up to a factor of 3.0 and 2.3, respectively (Nakićenović et al., 2000). Although the suite of IPCC SRES emissions projections are highly variable and uncertain, nearly all of the estimates predict an increase in ozone precursor emissions through the 2050's. It is already well documented that global ozone concentrations have increased significantly over the past century due to increased anthropogenic emissions (Marenco et al., 1994; Staehelin et al., 1994; Varotsos and Cartalis, 1991). As these emissions continue to increase, ozone related air quality issues can be expected to become more pronounced. In regions such as the west coast of North America, there is already evidence that regional air quality is influenced by increasing global anthropogenic emissions, and in particular, increasing Asian emissions. Jaffe et al. (2003) found that surface and airborne measurements of ozone in the springtime air transported from the Eastern Pacific to the west coast of the US showed ozone increasing by 30% (approximately 10 ppbv) from the mid 1980's to 2002. Similarly, Vingarzan and Thomson (2004) observed an increase of approximately 3.5 ppbv in the ozone levels of marine air transported into Southwestern British Columbia from 1991 to 2000, due to a combination of increased global background levels and direct influence from Asian emissions.

Changes in biogenic emissions are also expected to play a key role in determining future air quality. Climate influences biogenic volatile organic compound (BVOC) emissions primarily by temperature and solar radiation, and to a lesser extent precipitation patterns and soil moisture distributions. Consequently, changes in climate may have a profound impact on regional BVOC emissions. In addition, BVOC emissions may also be influenced through human forces such as urbanization and land management practices, as well as naturally through climate driven changes in regional vegetative patterns (Constable et al., 1999; Wiedinmyer et al., 2006; Heald et al., 2008). Changes in atmospheric chemical composition, including carbon dioxide and ozone, can also modify biogenic VOC emissions (Guenther et al., 2006).

Recent modeling studies have shown the importance of an integrated approach to studying the impacts of global changes on regional air quality. Hogrefe et al. (2004b) investigated the impact of global changes (IPCC A2 scenario) in the 2050's on regional air quality in the Eastern US, and found that summertime average daily maximum 8-h ozone concentrations were most significantly influenced by changes in chemical boundary conditions (+5.0 ppb) followed by meteorological changes (+4.2 ppb) and anthropogenic emissions (+1.3 ppb). The work of Steiner et al. (2006) investigated the impact of changes in climate and emissions reductions on ozone levels in central California, and found that projected reductions in anthropogenic emissions has the single largest impact on air quality, reducing ozone by 8–15% in urban areas, while climate change is projected to increase ozone 3–10%. Tagaris et al. (2007) found that the projected impact of climate change on US air quality in the 2050's is small compared to the impact of control-related reductions in emissions, and that the combined effect of climate change and emissions leads to a decrease in mean summertime daily maximum 8-h ozone of 20% and a reduction of 23% in the mean annual $PM_{2.5}$ concentration. Similarly, Wu et al. (2008) determined that the large emissions reductions in the IPCC A1B scenario would reduce mean summer daily maximum 8-h ozone by 2–15 ppb in the Western US and 5–15 ppb in the east, while the associated climate change would increase ozone by 2–5 ppb over much of the United States. Liao et al. (2008) found that summertime US surface ozone would increase an additional 10 ppbv in many urban areas based on the A1B climate scenario.

Although it is known that the global environment is changing and that these changes may have a profound impact on air quality, the magnitude and spatial distribution of these impacts remain highly uncertain. In this work, we apply the EPA Community Multi-scale Air Quality (CMAQ) photochemical grid model (Byun and Schere, 2006) to examine the individual and combined impacts that global changes, projected to the 2050's, have on regional air quality in the United States. In a companion paper, Chen et al. (2008) present the overall modeling framework and examined the combined effects of global changes upon ozone in the US. In this paper, we take a comprehensive approach to examining how changes in future US ozone and $PM_{2.5}$ levels can be attributed to changes in climate, regional anthropogenic and biogenic emissions, global emissions (as chemical boundary conditions downscaled from a global chemical transport model), and land-use/land-cover through a matrix of sensitivity simulations. Section 2 briefly describes the methodology and models used in this study. In Sect. 3, we evaluate model performance with respect to observations and describe the attribution results, and in Sect. 4 we present our conclusions.

Table 1. Designated model inputs for the six attribution cases. The "present-day" parameters refer to input representative of the 1990's, while "future-2050" refers to input parameters representative of the 2050's. Each case is comprised of five separate month long simulations representative of July meteorological conditions.

Simulation Name	Chemical boundary conditions	Anthropogenic emissions	Land-use/land-cover	Meteorology
CURall	present-day	present-day	present-day	present-day
FUTall	future-2050	future-2050	future-2050	future-2050
futBC	future-2050	present-day	present-day	present-day
futEMIS	present-day	future-2050	future-2050	present-day
futMETcurLU	present-day	present-day	present-day	future-2050
futMETfutLU	present-day	present-day	future-2050	future-2050

2 Methodology

In order to quantify the impact of projected global changes on surface ozone and $PM_{2.5}$ concentrations, we conducted a matrix of CMAQ attribution simulations based on six different combinations of model inputs (Table 1). Each of the six attribution cases were comprised of five separate month long simulations using meteorological conditions representative of July, for either present-day (1990–1999) or future (2045–2054) time periods. July conditions from five separate years were chosen based on modeled peak temperatures in order to fully cover the range of simulated temperatures, and to ensure our results were representative of average July conditions for each climate period. The future conditions were based on the IPCC SRES A2 "business as usual" scenario (Nakićenović et al., 2000). The scenario ranks as one of the more severe IPCC scenarios in terms of future population growth, temperature change, and increases in ozone and $PM_{2.5}$ precursor emissions.

We first simulated present-day levels of ozone and $PM_{2.5}$ with CMAQ driven by meteorology, chemical boundary conditions, anthropogenic emissions, and land-cover that reflect present-day conditions (CURall case). Future ozone and $PM_{2.5}$ were simulated using CMAQ driven by model inputs that reflect projected conditions for the 2045–2054 (hereafter referred to as future-2050) time period (FUTall case). To examine the individual effects of projected global change parameters on ozone and $PM_{2.5}$ concentrations, four additional attribution cases were simulated. Specifically, these four cases examined the impact of future chemical boundary conditions alone (futBC simulation), future anthropogenic emissions combined with future land-cover (futEMISfutLU simulation), future climate alone (futMETcurLU), and future climate combined with future land-cover (futMETfutLU). All modeling results were grouped and analyzed by EPA region (see Fig. 1). For simplicity, we have combined results from Regions 1, 2, and 3 designated as R1-3.
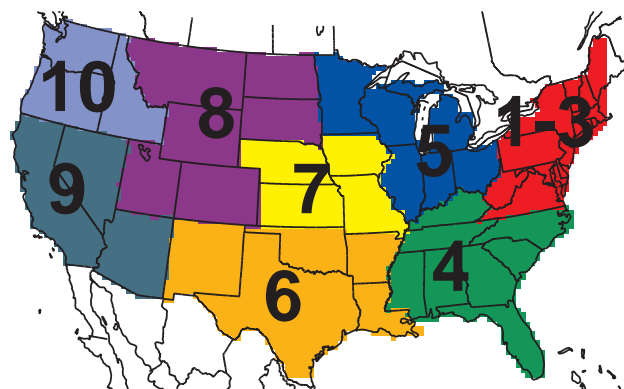

Fig. 1. EPA regions for the continental United States. Note that for simplicity Regions 1, 2, and 3 are treated as a single combined region (1-3).

2.1 Model setup

2.1.1 Chemical transport model

The modeling approach is similar to that described in Chen et al. (2008). The CMAQ version 4.4 photochemical grid model was run on a 36-km by 36-km gridded domain, centered over the continental US, with 17 vertical sigma levels from the surface to the tropopause. Gas-phase chemistry was modeled using the SAPRC-99 chemical mechanism (Carter 2000a, b). Aerosol processes were simulated using a modal approach with the AERO3 aerosol module (Byun and Schere, 2006), which includes the ISORROPIA secondary inorganic aerosol algorithms (Nenes et al., 1998) and the SORGAM secondary organic aerosol formulations (Schell et al., 2001). The AERO3 module contains process dynamics for nucleation, coagulation, condensation, evaporation and dry deposition (Binkowski et al., 2003). Aerosol species include sulfates, nitrates, ammonium, primary and secondary organics, and elemental carbon.
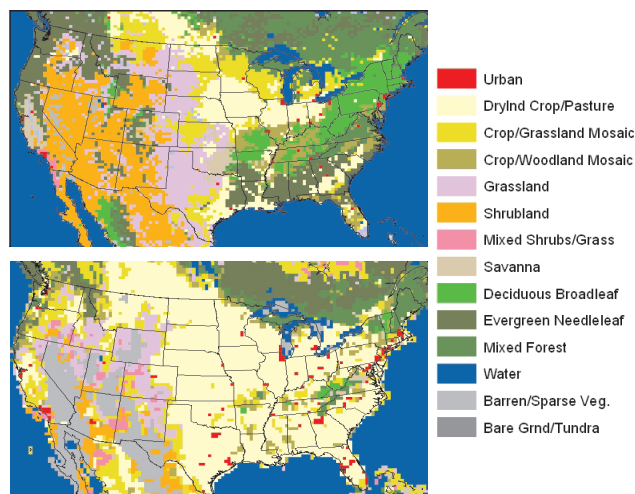
Fig. 2. MM5 land-use by USGS category for the present-day (top) and future-2050 (bottom) simulations.

2.1.2 Meteorology

To generate the meteorological fields for CMAQ, an MM5-based regional climate model (Salathé et al., 2008) was used to downscale present-day and future-2050 global climate model results from the NCAR-DOE Parallel Climate Model (PCM, Washington et al., 2000). The PCM model couples atmospheric, land surface, ocean, and sea-ice modules to form an earth system model for current and future climate scenario projections. The future-2050 PCM simulations were based on the IPCC A2 emission scenario.

The regional climate model is based on the Pennsylvania State University (PSU)-National Center for Atmospheric Research (NCAR) mesoscale model (MM5) Release 3.6.3 (Grell et al., 1994). Simulations were performed in non-hydrostatic mode with 28 vertical sigma levels, and a one-way nested configuration at 108-km and 36-km resolutions. In order to maintain simulation stability and mass conservation, nudging was employed towards the PCM output on the outer 108-km domain. This constrains MM5 to the global model and results in a smooth transition from the global model to the continental scale MM5 simulations.

The MM5 model configurations for the present-day and future-2050 simulations were identical except for the land-use data. Since variations in land-use are known to influence regional meteorology and air quality (Civerolo et al., 2000), land-use for the future-2050 simulations was updated with data prepared for the Community Land Model (CLM; Bonan et al., 2002), and the Spatially Explicit Regional Growth Model (SERGOM; Theobald, 2005). The SERGOM provided projected urban and suburban population density distributions, while the remaining land-use data was based on a preliminary mapping of plant functional type distributions for the CLM (J. Feddema, personal communications, 2006).
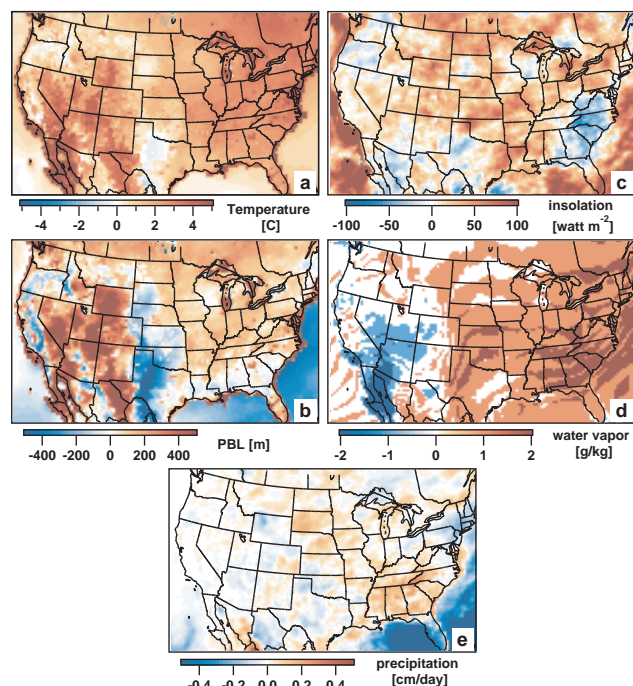

Fig. 3. Projected July changes from the present-day to the 2050's for **(a)** average daily maximum surface temperature, **(b)** average daily maximum boundary layer height, **(c)** average daily surface insolation, **(d)** average daily water vapor content within the boundary layer, and (e) average daily precipitation.

These maps were based on an interpolation of the Integrated Model to Assess the Global Environment (IMAGEv2.2; Alcamo et al, 1998; Nakićenović et al., 2000; RIVM, 2002; Strengers et al., 2004). A cross-walk was created to map the CLM land cover plant functional types together with the urban land cover from SERGOM to the MM5 land-use and land-cover categories. Future land-use held natural vegetation constant relative to the present-day land cover dataset, but the natural vegetation was reduced due to simulated agriculture and grazing represented by the IMAGE 2.2 SRES A2 scenario. Figure 2 depicts the land-use for the present-day and future-2050 simulations. The future land-use maps are dominated by agriculture (shrubs, grasslands and dry-land crops) with large reductions in evergreen forests and wooded wetlands.

Projected changes in average July daily maximum (DM) surface temperature, boundary layer height, downward solar radiation, and daily accumulated precipitation, as well as average water vapor content within the boundary layer are shown in Fig. 3. Differences are computed as the 5-year July average in the future simulation minus the present-day simulation. Average DM surface temperatures are projected to increase across the continental US, however, the magnitude of the increase varies greatly by region. The Eastern US is expected to have the largest increase in average DM surface

temperature, with Region 1–3 having a projected increase of +3.4°C and Region 4 projected to increase by +2.6°C. The Western US (Region 9) shows comparable changes with Region 4, while the Pacific Northwest (Region 10) shows the smallest increase in average DM surface temperature of approximately +1.0°C. The July average DM PBL height is projected to increase by approximately 100 m or more for most regions, except Regions 6 and 7, which show only slight increases due to offsetting changes in PBL heights within the two regions. In the western half of the US, changes in DM PBL height are directly related to changes in DM surface temperature, where regions with smaller changes in surface temperature (e.g., Texas, California, Oregon) show decreases in PBL heights, and regions with the largest increase in temperature (southwestern states) correspond to the largest increase in PBL height. In the eastern half of the US, the direct relationship between DM PBL heights and DM surface temperature is generally true for the Midwest (excluding parts of Wisconsin) and northeast (excluding parts of New England), while the opposite is true for much of the southeast (excluding most of Florida). In regions where increases in PBL height correspond to increases in temperature, any reduction in air quality due to increased temperatures may be somewhat offset by increases in PBL heights. However, in regions such as the southeast, where reductions in PBL height occur simultaneously with increases in temperature, changes in both meteorological parameters will tend to reduce air quality. Note that the larger increases in temperature and PBL heights along the coastlines are due to a slight mismatch in the land surface classifications for the present-day and future-2050 scenarios, and are not the result of climate change. The mismatch in land surface classifications does not imply the meteorology is misrepresented in the future-2050 simulations, only that the land-ocean interface has been shifted by one grid cell. The shift has little impact on our overall results because inland grid cells are not affected by whether or not the coast line is one grid cell further away.

The general trend for July surface insolation is a future increase for much of the US due to reduced cloud cover. This implies faster photolysis rates in the atmosphere leading to increased production of photo-reactive pollutants such as ozone. There are, however, regions such as portions of Texas, the Pacific Northwest, and the Southeastern US, which are projected to experience a decrease in surface insolation at the surface due to increased cloud cover, potentially leading to improved air quality in those regions.

Water vapor content is generally projected to increase in the Eastern US, while the Western US shows small regions of slight increases combined with larger areas of decreasing water vapor content. Increases in water vapor in relatively clean environments (i.e., low NO_x) are generally expected to decrease ozone due to the destruction of ozone through photolysis and the removal of the $O(^1D)$ molecule via $O(^1D)+H_2O\rightarrow2OH$ (Stevenson et al., 2000), as well as through the reaction $O_3+HO_2 \rightarrow2O_2+OH$ (Racherla and

Adams, 2008). In NO_x polluted environments, increased water vapor is expected to increase ozone through the competing reaction $NO+HO_2 \rightarrow NO_2+OH$ (Racherla and Adams, 2008). The largest changes in precipitation are projected to occur in the southeast, which will increase removal of pollutants through wet deposition. Smaller increases in precipitation are projected in the northwest and north central regions, while the west central states are generally projected to experience a decrease in precipitation.

2.1.3 Chemical boundary conditions

Both present-day and future-2050 sets of chemical boundary conditions were obtained through the downscaling of output from the MOZART-2 (Model for Ozone and Related Chemical Tracers, version 2.4) global chemical transport model. The MOZART-2 output used in this work is described by Horowitz (2006). Horowitz (2006) applied MOZART-2 to estimate tropospheric ozone and aerosol concentrations from 1860 to 2100 based on historical and projected changes in emissions, while the feedbacks from climate change and trends in stratospheric ozone were ignored. The historical simulations (1860–1990) were based on the EDGAR-HYDE historical emissions inventory (van Aardenne et al., 1999), while the future simulations (1990–2100) were based on emissions projections from four different IPCC SRES scenarios (A2, A1B, B1, and A1F1). For the purpose of this work, we obtained daily average model results from the IPCC SRES A2 simulations, for July 2000 and July 2050. Note that the meteorological inputs used to drive the MOZART-2 simulations are not the same as the PCM results used in this work, so some consistency is lost. However, the MOZART-2 output does provide a representative set of present-day and projected future-2050 chemical boundary conditions for the CMAQ simulations. Generally, for all four boundaries MOZART-2 predicts an increase in ozone of approximately 10 ppbv from the present-day to future-2050 conditions, while NO_x and NO_y ($NO+NO_2+HNO_3+N_2O_5+PAN+HNO_4+$other organic nitrates) increase by approximately 10 pptv and 130 pptv, respectively (larger increases, 60 pptv and 230 pptv, were observed along the southern boundary). NMVOCs increase approximately 0.7 ppbv, while $PM_{2.5}$ increased approximately $0.8 \mu g\,m^{-3}$ along the western and southern boundaries, reflecting projected increases in particulate and precursor emissions from Asia and South America. Little to no change in $PM_{2.5}$ is projected along the northern and eastern boundaries.

2.1.4 Regional emissions

The anthropogenic emissions inventory used in this work is based on the 1999 EPA National Emissions Inventory (NEI-1999), and was processed through the SMOKE (Sparse Matrix Operating Kernel Emissions; Houyoux et al., 2005) emissions system. Future anthropogenic emissions were

Table 2. Summary of US total present-day and projected future-2050 anthropogenic and biogenic emissions for the month of July. Fractional change (future-2050 / present-day) is shown in parentheses for anthropogenic emissions.

species	units	anthropogenic				biogenic			
		point	area	non-road	mobile	present meteorology, present land-cover	present meteorology, future land-cover	future meteorology, present land-cover	future meteorology, future land-cover
CO		11.4 (1.0)	40.2 (1.20)	72.5 (1.11)	161.4 (0.99)	–	–	–	–
NO_x		24.1 (1.0)	3.7 (1.58)	12.6 (1.10)	22.4 (0.99)	4.1	4.1	4.2	4.2
VOC		4.5 (1.0)	19.9 (2.11)	8.1 (1.30)	15.6 (0.98)	156	96	188	103
NH_3	ktons/day	0.2 (1.0)	15.2 (2.50)	0.01 (1.06)	0.8 (0.99)	–	–	–	–
SO_2		42.7 (1.0)	2.8 (1.57)	1.5 (1.33)	0.8 (0.99)	–	–	–	–
PM_{10}		4.5 (1.0)	57.1 (1.93)	1.1 (1.17)	0.7 (0.99)	–	–	–	–
$PM_{2.5}$		3.6 (1.0)	13.9 (1.79)	1.0 (1.17)	0.5 (0.99)	–	–	–	–

projected based on emission growth factors from the EPA Economic Growth Analysis System (EGAS; US EPA, 2004) and extrapolated to 2050 using assumptions consistent with the IPCC A2 scenario. Future emissions accounted for estimated population and economic growth, as well as projected energy use by sector. Future emissions did not include recent emission control regulations or major technology breakthroughs that would affect the use of traditional energy. Future mobile sources emissions were generated through EGAS based on estimated MOBILE6 VMT growth rates. Mobile emissions estimates considered increases in alternative fuel vehicles and decreases in old vehicle fleets, but the dominant transportation fuels remain gasoline and diesel. The EGAS growth factors were applied to area and mobile source categories, but not to point sources. Future anthropogenic emissions were also updated to account for the expansion of urban areas through projected population and housing distributions by the SERGOM model for the year 2030. Present-day and projected future-2050 anthropogenic emissions are summarized in Table 2. Area source emissions are projected to experience the largest increase, with emissions for all species, excluding CO, increasing by more than 50%. Non-road emissions are projected to increase between 6% and 33%, depending on the species, while mobile emissions are projected to remain relatively unchanged.

Biogenic emissions were generated dynamically using MEGAN (Model of Emissions of Gases and Aerosols from Nature; Guenther et al., 2006) with the parameterized form of the canopy environment model. The model estimates hourly isoprene, monoterpene, and other BVOC emissions based on plant functional type and as a function of hourly temperature and ground level shortwave radiation from MM5. Satellite observations of leaf area are used to estimate monthly emission variations associated with leaf age and foliar density. For the current land-cover case, a 1-km seasonal vegetation dataset, derived from satellite and ground observations, was used. For the future-2050 land-cover case, the vegetation dataset was based on the same CLM projected land-cover data used in the MM5 simulations described above (Fig. 2). The CLM land-cover data includes percent coverage of plant functional type and MEGAN includes emission factors based
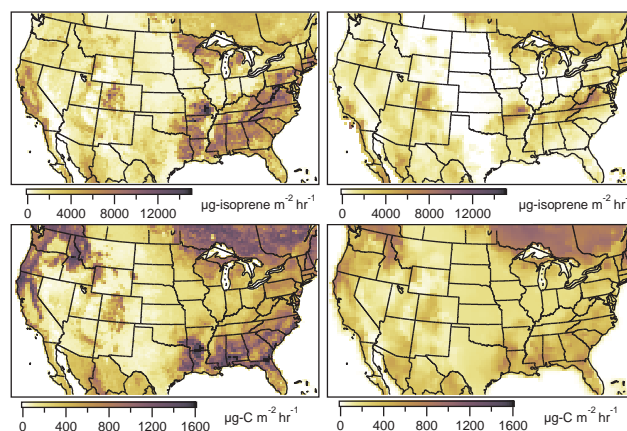
Fig. 4. Biogenic emissions capacity maps (normalized to 30°C and 1000 μmoles m^{-2} s^{-1} photosynthetically active radiation) for **(a)** present-day isoprene, **(b)** present-day monoterpenes, **(c)** future-2050 isoprene, and **(d)** future-2050 monoterpenes.

on plant functional type. For the future-2050 case, MEGAN emission factors were assigned based on the CLM percent cover of plant functional type for a given grid cell.

Projected changes in land-cover resulted in large changes in biogenic emissions capacity from the present-day to future-2050 case (Fig. 4). In the future, isoprene emitting vegetation has been reduced in the south and south eastern states, as well as in the northern mid-west and along the west coast of California. Similarly, a reduction of monoterpene emitting plants is projected along the west coast of the US and into Southern Canada, as well as in the South and Southeastern US and Eastern Canada. The projected reduction of isoprene and monoterpene emitting plants is sufficient to negate any increase in emissions due to increased future temperatures, and results in a net reduction in total future-2050 BVOC emissions compared to the present-day. This work does not include projected changes in biogenic nitrogen emissions due to increased croplands or changes in management practices in regards to the application of fertilizers. Table 2 includes a comparison of total continental US biogenic emissions used in the attribution cases: present-day
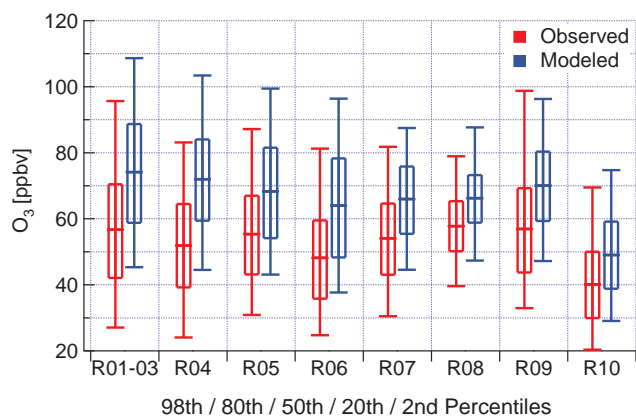
Fig. 5. Comparison of modeled to observed daily maximum 8-h ozone concentrations.

Fig. 6. Comparison of modeled to observed average 24-h (A24-h) $PM_{2.5}$ concentrations.

land-cover with present-day meteorology (CURall and futBC cases), future-2050 land-cover with present-day meteorology (futEMIS case), present-day land-cover with future-2050 meteorology (futMETcurLU case), and future-2050 land-cover with future-2050 meteorology (FUTall and futMET-futLU cases).

3 Results and discussion

In the following sections, we first compare simulated surface ozone and $PM_{2.5}$ concentrations from the present-day (CU-Rall) simulations to measurements made at monitoring sites throughout the United States. We then analyze and discuss the results of our attribution CMAQ simulations in terms of daily maximum 8-h (DM8H) ozone and average 24-h (A24-h) $PM_{2.5}$ concentrations.

3.1 Ozone and $PM_{2.5}$ evaluation

CMAQ has undergone extensive evaluation for both ozone and $PM_{2.5}$ model predictions for the continental US (e.g. Eder and Yu, 2006; Phillips and Finkelstein, 2006), and has shown good performance for most regions. CMAQ model evaluations for simulations using downscaled climate model output are limited, but suggest that CMAQ is a suitable tool for use in climate impacts on air quality studies. Hogrefe et al. (2004a) found that CMAQ performed best for predicting patterns of average and above average ozone concentrations, as well as the frequency distribution of extreme ozone events. Tagaris et al. (2007) found mean 8-h ozone concentrations were approximately 15% higher than observations, while $PM_{2.5}$ concentrations were approximately 30% lower than observed. Furthermore, Tagaris et al. (2007) found that $PM_{2.5}$ model performance is significantly more region specific than mean 8-h ozone performance.
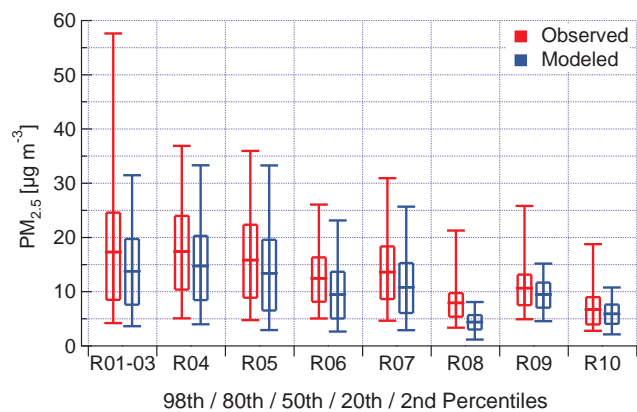
Model performance is evaluated through a comparison of modeled and observed DM8H ozone and A24-h $PM_{2.5}$ concentrations (Figs. 5 and 6). Since our CMAQ simulations were driven by MM5 results that were nudged towards climate model output and not observations, our present-day (CURall) simulations represent a realization of present-day air quality and are not representative of air quality at any specific time (i.e., we cannot do a direct day-to-day or hour-to-hour comparison with observations).

Hourly ozone and daily $PM_{2.5}$ observations were obtained from the EPA AQS database for the five July's from 1999–2003. A total of 1349 ozone and 1277 $PM_{2.5}$ monitoring sites were used. Figure 5 compares ranked modeled and observed DM8H ozone concentrations averaged across all sites within each EPA region. Model performance for average DM8H ozone is fairly consistent across all regions, ranging from an over-prediction of +15% in Region 8 to +39% in Region 4. Peak DM8H ozone, represented by the 98th percentile value, shows better performance than the average, and ranges from −2% in Region 9 to +24% in Region 4. Figure 6 compares ranked modeled and observed A24-h $PM_{2.5}$ concentrations averaged across all sites within each EPA region. Modeled A24-h $PM_{2.5}$ performance is relatively consistent across all regions, ranging from an under-prediction of −11% in Region 9 to −24% in Region 6. The only exception to this is in Region 8, which under-predicts the average by −44%. The peak (98th percentile) 24-h $PM_{2.5}$ concentrations show much more variability compared to the average, and range from under-predictions of −7% to −17% for Regions 4, 5, 6, and 7 to under-predictions of −41% to −62% in Regions 1–3, 8, 9, and 10. These results are consistent with those from our companion paper (Chen et al., 2008) which addressed model performance for ozone for periods extending beyond the July period considered here.
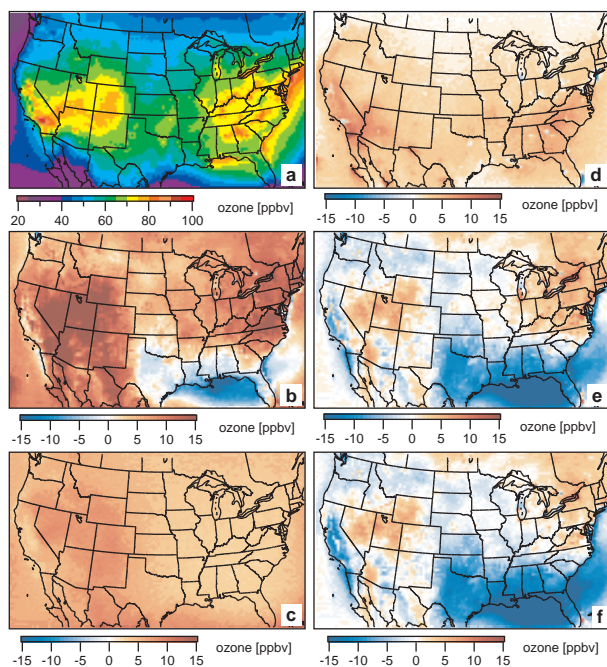
Fig. 7. Average daily maximum 8-h ozone for **(a)** the CURall sim-
ulation, **(b)** difference between the FUTall and CURall simulations,
(c) difference between the futBC and CURall simulations, **(d)** dif-
ference between the futEMIS and CURall simulations, **(e)** differ-
ence between the futMETcurLU and CURall simulations, and **(f)**
difference between the futMETfutLU and CURall simulations.

3.2   Ozone results

The impact of projected future-2050 global changes on sur-
face ozone concentrations is spatially highly variable. Some
regions experience increases in ozone greater than 10 ppbv
(West-Central US), while others see reductions of a few ppbv
(Southeastern US). Figure 7 shows a map of the average
DM8H ozone concentration for the CURall base case sim-
ulation with difference maps for the five attribution simula-
tions. Results are summarized by EPA region in Table 3. Fur-
ther analysis of the impact of the combined effects of global
change upon summertime ozone is given in a companion pa-
per by Chen et al. (2008).

On average, projected changes in chemical boundary con-
ditions (futBC simulation) have the largest impact on US av-
erage DM8H ozone levels (+5 ppbv). The boundary condi-
tion impact is more pronounced in the west (+6 ppbv) than
in the east (+4 ppbv), due to the predominant westerly flow
across the US. As a result, as distance increases from the
western boundary, the the boundary conditions have less ef-
fect upon ozone levels. These results are consistent with
Hogrefe et al. (2004b) who showed that changes in chemi-
cal boundary conditions following the IPCC A2 scenario had
the largest impact on ozone levels.

Future emissions changes (futEMIS) are projected to in-
crease average DM8H ozone levels across the US by an av-

erage of +3 ppbv. The largest increases in average DM8H
ozone are projected to occur in regions that combine in-
creases in anthropogenic emissions with sufficient biogenic
emissions. In particular, Region 9 in the west and Region 4
in the southeast show the largest increase in average DM8H
ozone (+5 ppbv). The smallest increase in average DM8H
ozone (+2 ppbv) occurs in Regions 5 and 8, which com-
bine relatively smaller increases in anthropogenic emissions
with lower future biogenic emissions. Hogrefe et al. (2004b)
project a smaller increase in ozone due to future anthro-
pogenic emissions with an increase of only 1.3 ppbv in the
Eastern US. The discrepancy between Hogrefe et al. (2004b)
and the results presented here is most likely due to differ-
ences in how future regional anthropogenic emissions are
projected. Hogrefe et al. (2004b) projected future US emis-
sions based on the IPCC A2 scenario, while emissions in this
work are projected using the EPA EGAS model. In con-
trast, Tagaris et al. (2007) found that under the A1b sce-
nario a simulated 20% reduction in ozone was primarily due
to control-related reductions in emissions within the United
States. Similarly, Tao et al. (2007) found that under the
IPCC B1 scenario, a projected 4–12% reduction in ozone was
dominated by emissions changes, while Steiner et al. (2006)
found that projected reductions in California's anthropogenic
emissions had the single largest effect on reducing ozone.

Projected meteorological changes (futMETcurLU simula-
tion) result in an overall decrease (−1.3 ppbv) in US average
DM8H ozone. Meteorological impacts are spatially highly
variable. The largest increases in average DM8H ozone (ap-
proximately +4 ppbv), are found in the northeast and west
central regions. Our results for the northeast are in agree-
ment with Hogrefe et al. (2004b) who found that climate
change resulted in an increase of roughly 4 ppbv in aver-
age DM8H ozone, as well as, Racherla and Adams (2008)
who found that climate change based on the A2 scenario in-
creased 95th percentile ozone in the Eastern US by approxi-
mately 5 ppbv. In the west central region, increased temper-
ature and reduced cloud cover may be somewhat offset by
increases in daytime PBL height, but the overall result is an
increase in average DM8H ozone. In the northeast, increased
average DM8H ozone appears to be due to a combination of
increased temperature with only small increases in daytime
PBL heights, as well as decreased cloud cover. The largest
decreases in average DM8H ozone appear in the south and
southwestern regions (−6 ppbv), with smaller decreases oc-
curring along the west coast and northern regions (approxi-
mately −1 ppbv). The smaller decrease along the west coast
is in contrast with Steiner et al. (2006) who found that cli-
mate change alone would increase ozone 3-10% throughout
California. The large decrease in the south and southeast-
ern regions is most likely the result of increased convective
precipitation, which enhances the removal of organic nitrates
and other reactive nitrogen species, reducing the amount of
reactive nitrogen available to participate in ozone chemistry.

Table 3. Average daily maximum 8-h ozone (ppbv) averaged across EPA region for each simulation.

EPA Region	CURall	FUTall	futBC	futEMIS	futMETcurLU	futMETfutLU
R1-3	70	+12	+4	+3	+4	+2
R04	70	+3	+3	+5	−5	−8
R05	63	+7	+4	+2	+1	+0
R06	63	+3	+5	+3	−6	−7
R07	61	+5	+4	+3	−1	−2
R08	62	+9	+6	+2	+0	+0
R09	68	+12	+6	+5	+0	−1
R10	53	+7	+6	+3	−1	−1
US	64	+7	+5	+3	−1.3	−2.6

When projected changes in future land-use are combined with future meteorological conditions (futMETfutLU case), the future average DM8H ozone is spatially very similar to when only meteorological changes are considered (fut-METcurLU case). Accounting for changes in future land-use (i.e., reduced biogenic emissions) has the effect of enhancing the projected decrease in average DM8H ozone. This enhancement is most pronounced in Region 4, where the largest decreases in BVOC emissions are projected. In Region 4, average DM8H ozone is estimated to decrease an additional 3 ppbv from −5 ppbv to −8 ppbv. On average across the US, the decrease in average DM8H ozone is projected to double from −1.3 ppbv, when climate change alone is considered, to −2.6 ppbv when climate change and future land-use changes are accounted for simultaneously.

The combined effects of projected changes in chemical boundary conditions, emissions, land-use, and climate (FU-Tall simulation) on average DM8H ozone results in the largest increases in the West Central US (e.g., +12 ppbv in Region 9, California) and in the Northeastern US (e.g., +12 ppbv in Region 1–3). In Region 1–3, all of the global changes accounted for in this study lead to increases in average DM8H ozone. The same is true for the eastern portion of Region 9. However, in the western portion of Region 9, changes in chemical boundary conditions and emissions both increase average DM8H ozone, while climate changes have the opposite effect. The largest projected decreases in average DM8H ozone occur in the south and southeast regions, where future average DM8H ozone is dominated by climate effects. This is reflected in the relatively small increases in average DM8H ozone (+3 ppbv) in Regions 4 and 6. On average across the US, the combined effects of projected global changes result in a +7 ppbv increase in average DM8H ozone, and the changes in ozone are dominated by changes in chemical boundary conditions and emissions in most regions, except for the southeast, which is dominated by changes in convective precipitation.
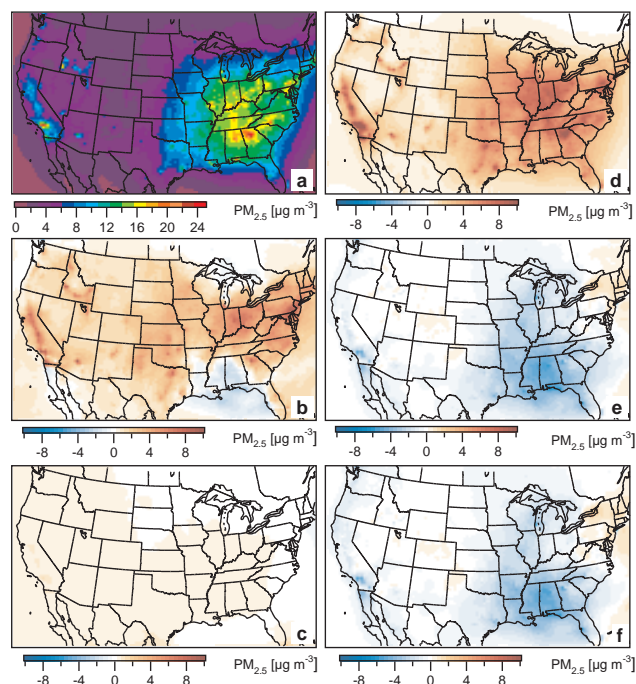

Fig. 8. Average 24-h PM$_{2.5}$ concentration for **(a)** the CURall simulation, **(b)** difference between the FUTall and CURall simulations, **(c)** difference between the futBC and CURall simulations, (d) difference between the futEMIS and CURall simulations, **(e)** difference between the futMETcurLU and CURall simulations, and **(f)** difference between the futMETfutLU and CURall simulations.

3.3 PM$_{2.5}$ results

Simulated July A24-h total PM$_{2.5}$ results are shown in Fig. 8 and summarized in Table 4. Results for speciated PM$_{2.5}$ mass are summarized in Tables 4, 5, 6, and 7. Changes in emissions (futEMIS case) contribute the most to increasing A24-h PM$_{2.5}$ concentrations across the US (approximately +3 μg m^{-3}). Under the futEMIS case, all speciated PM components, except for secondary organic aerosol (SOA), contribute to increasing PM$_{2.5}$ mass. SOA is reduced in most

Table 4. Average 24-h concentration ($\mu g\,m^{-3}$) for total PM$_{2.5}$ and speciated sulfate (SO$_4$) mass averaged across EPA region for each simulation.

| EPA Region | Total PM$_{2.5}$ | | | | | | SO$_4$ | | | | | |
	CUR all	FUT all	fut BC	fut EMIS	futMETcurLU	futMET futLU	CUR all	FUT all	fut BC	fut EMIS	futMETcurLU	futMET futLU
R1-3	11	+4	+0.0	+4	+0.2	+0.4	5.0	+0.9	−0.1	+0.7	+0.0	+0.6
R04	13	+1	+0.3	+5	−3	−3	6.1	−0.6	+0.2	+1.2	−1.8	−1.1
R05	10	+3	+0.2	+5	−1	−1	4.1	−0.1	+0.1	+0.6	−0.8	−0.5
R06	6	+2	+0.4	+3	−1	−1	2.6	+0.0	+0.2	+0.6	−0.7	−0.6
R07	8	+3	+0.3	+4	−1	−1	3.0	+0.0	+0.1	+0.6	−0.7	−0.5
R08	3	+2	+0.3	+1	+0	+0	1.0	+0.4	+0.2	+0.2	+0.0	+0.0
R09	5	+2	+0.6	+2	−0.4	−0.5	1.5	+0.4	+0.3	+0.2	−0.1	−0.1
R10	4	+2	+0.5	+1	−0.2	−0.4	1.2	+0.3	+0.3	+0.1	−0.1	−0.1
US	7	+2	+0.4	+3	−0.9	−0.8	2.9	+0.1	+0.2	+0.5	−0.5	−0.3

Table 5. Average 24-h concentration ($\mu g\,m^{-3}$) for speciated nitrate (NO$_3$) and ammonium (NH$_4$) mass averaged across EPA region for each simulation.

| EPA Region | NO$_3$ | | | | | | NH$_4$ | | | | | |
	CUR all	FUT all	fut BC	fut EMIS	futMETcurLU	futMET futLU	CUR all	FUT all	fut BC	fut EMIS	futMETcurLU	futMET futLU
R1-3	0.2	+0.8	+0.0	+1.0	−0.1	+0.0	1.5	+0.9	+0.0	+0.8	+0.0	+0.1
R04	0.1	+0.7	+0.0	+1.1	−0.1	+0.0	1.9	+0.3	+0.1	+1.1	−0.5	−0.3
R05	0.3	+0.7	+0.0	+1.3	−0.1	−0.1	1.4	+0.3	+0.1	+0.7	−0.3	−0.2
R06	0.1	+0.3	+0.0	+0.4	+0.0	+0.0	0.9	+0.1	+0.1	+0.4	−0.2	−0.2
R07	0.3	+0.6	+0.0	+0.9	−0.1	−0.1	1.2	+0.2	+0.1	+0.5	−0.3	−0.2
R08	0.1	+0.2	+0.0	+0.2	+0.0	+0.0	0.4	+0.2	+0.1	+0.1	+0.0	+0.0
R09	0.2	+0.3	+0.0	+0.5	−0.1	−0.1	0.6	+0.2	+0.1	+0.2	−0.1	−0.1
R10	0.1	+0.1	+0.0	+0.2	+0.0	+0.0	0.4	+0.2	+0.1	+0.1	+0.0	+0.0
US	0.2	+0.4	+0.0	+0.6	−0.1	+0.0	1.0	+0.3	+0.1	+0.5	−0.2	−0.1

regions due to decreased biogenic emissions from projected changes in land-cover and from increased production of sulfate (SO$_2$), nitrate (NO$_3$), and ammonium (NH$_4$) aerosols, which reduces the OH radicals available for SOA production. The largest emissions induced increases in A24-h PM$_{2.5}$ are found in the East and Central US (+4 $\mu g\,m^{-3}$ for Regions 1–3 and 7; +5 $\mu g\,m^{-3}$ for Regions 4 and 5), while the smallest changes occur in the west (+1 $\mu g\,m^{-3}$ for Regions 8 and 10; +2 $\mu g\,m^{-3}$ for Region 9). Unlike ozone, changes in chemical boundary conditions (futBC case) have very little impact on PM$_{2.5}$ concentrations. A24-h PM$_{2.5}$ concentrations are influenced most by changes in chemical boundary conditions along the west coast (Regions 9 and 10). For all regions the increase in A24-h PM$_{2.5}$ is less than +1 $\mu g\,m^{-3}$, with the largest contribution coming from increases in SO$_4$ and NH$_4$ mass.

Changes in meteorology (futMETcurLU simulation) result in a slight decrease in A24-h PM$_{2.5}$ concentrations across the US (approximately −1 $\mu g\,m^{-3}$). The largest decrease in A24-h PM$_{2.5}$ occurs in Region 4 (−3$\mu g\,m^{-3}$), and is primarily due to enhanced precipitation throughout the region and the resulting increase in wet deposition of SO$_4$ and NH$_4$. Changes in PM$_{2.5}$ levels across the rest of the US range from +0.2 $\mu g\,m^{-3}$ in Region 1–3 to -1 $\mu g\,m^{-3}$ in Regions 5, 6, and 7. Overall, all speciated PM$_{2.5}$ concentrations either decline or remain the same under a future climate, except for

SOA and unspecified PM, which show small increases (0.1-−0.2 $\mu g\,m^{-3}$) in Region 1–3.

Results for the future meteorology and future land-use simulations (futMETfutLU case) show only a slight increase in A24-h PM$_{2.5}$ compared to the future meteorology and current land-use simulations (futMETcurLU case), which suggests that for A24-h PM$_{2.5}$, meteorological changes are more important than potential changes in future biogenic emissions due to land-use changes. The differences in results from the futMETfutLU and futMETcurLU cases are primarily due to a decrease in total BVOC emissions (see Fig. 4) and a spatial redistribution of those emissions due to changes in land-cover type (see Fig. 2) in the futMETfutLU case. This decrease in BVOC emissions leads to reduced SOA formation and enhanced OH levels, particularly in the east and southeastern regions. The enhanced OH subsequently leads to increases in SO$_4$, NO$_3$, and NH$_4$ aerosols compared to the futMETcurLU case. The increase in inorganic aerosol concentrations offsets the decrease in biogenic SOA, resulting in a small overall increase in A24-h PM$_{2.5}$ for the futMETfutLU case compared to the futMETcurLU case.

In the FUTall case, A24-h PM$_{2.5}$ concentration is projected to increase by +2 $\mu g\,m^{-3}$ across the continental US, with the largest increase projected to occur in Region 1–3 (+4 $\mu g\,m^{-3}$). Inorganic PM species SO$_4$, NO$_3$, NH$_4$, and unspecified PM mass contribute the most to increasing A24-h

Table 6. Average 24-h concentration (μg m^{-3}) for speciated elemental carbon (EC) and organic carbon (OC) mass averaged across EPA region for each simulation.

EPA Region	EC						OC					
	CUR all	FUT all	fut BC	fut EMIS	futMETcurLU	futMET futLU	CUR all	FUT all	fut BC	fut EMIS	futMETcurLU	futMET futLU
R1-3	0.3	+0.1	+0.0	+0.1	+0.0	+0.0	1.0	+0.3	+0.0	+0.2	+0.0	+0.0
R04	0.3	+0.1	+0.0	+0.1	+0.0	+0.0	1.1	+0.1	+0.0	+0.3	−0.2	−0.2
R05	0.3	+0.1	+0.0	+0.1	+0.0	+0.0	0.8	+0.2	+0.0	+0.2	−0.1	−0.1
R06	0.2	+0.0	+0.0	+0.0	+0.0	+0.0	0.6	+0.1	+0.1	+0.2	−0.1	−0.1
R07	0.2	+0.0	+0.0	+0.0	+0.0	+0.0	0.6	+0.1	+0.0	+0.2	−0.1	−0.1
R08	0.2	+0.0	+0.0	+0.0	+0.0	+0.0	0.7	+0.2	+0.0	+0.1	+0.0	+0.0
R09	0.4	+0.1	+0.0	+0.1	+0.0	+0.0	1.4	+0.4	+0.1	+0.3	+0.0	+0.0
R10	0.3	+0.1	+0.0	+0.0	+0.0	+0.0	1.1	+0.4	+0.1	+0.3	+0.0	+0.0
US	0.3	+0.1	+0.0	+0.1	+0.0	+0.0	0.9	+0.2	+0.0	+0.2	−0.1	−0.1

Table 7. Average 24-h concentration (μg m^{-3}) for speciated secondary organic aerosol (SOA) and unspecified mass averaged across EPA region for each simulation.

EPA Region	SOA						unspecified mass					
	CUR all	FUT all	fut BC	fut EMIS	futMETcurLU	futMET futLU	CUR all	FUT all	fut BC	fut EMIS	futMETcurLU	futMET futLU
R1-3	1.0	−0.3	+0.0	−0.3	+0.1	−0.4	1.9	+1.4	+0.0	+1.1	+0.2	+0.2
R04	1.2	−0.6	+0.0	−0.4	−0.3	−0.7	2.4	+1.4	+0.0	+1.8	−0.2	−0.2
R05	0.5	−0.1	+0.0	−0.1	−0.1	−0.2	2.4	+1.9	+0.0	+2.0	−0.1	−0.1
R06	0.3	−0.2	+0.0	−0.1	−0.1	−0.2	1.6	+1.3	+0.0	+1.5	−0.1	−0.1
R07	0.2	−0.1	+0.0	+0.0	−0.1	−0.1	2.1	+1.9	+0.0	+2.0	+0.0	+0.0
R08	0.1	+0.0	+0.0	+0.0	+0.0	+0.0	0.7	+0.6	+0.0	+0.6	+0.0	+0.0
R09	0.3	+0.0	+0.0	+0.0	+0.0	−0.1	1.0	+0.8	+0.0	+0.9	−0.1	−0.1
R10	0.5	−0.1	+0.0	−0.1	+0.0	−0.2	0.8	+0.7	+0.0	+0.8	+0.0	+0.0
US	0.5	−0.2	+0.0	−0.1	−0.1	−0.2	1.5	+1.2	+0.0	+1.3	−0.1	−0.1

PM$_{2.5}$ both in Region 1–3 and for the US as a whole, while changes in SOA tend to reduce PM levels in all regions. The smallest increase in A24-h PM$_{2.5}$ is projected to occur in Region 4 (+1 μg m^{-3}), where reductions in SOA are largest and increased precipitation leads to enhanced removal of PM through wet deposition.

4 Conclusions

Changes in future ozone and PM$_{2.5}$ concentrations compared to the present-day, are due to the synergistic effects of changes in chemical boundary conditions, regional anthropogenic emissions, land-use/land-cover (biogenic emissions), and climate. We have presented a comprehensive approach to addressing the individual and combined effects of these global changes on future US air quality through the off-line coupling of global and regional climate, chemical transport, and emissions models. Although other work has addressed the impact of various global changes on air quality, to our knowledge, this is the first study to address a number of these global changes in such a comprehensive manner.

Overall, US July average DM8H ozone concentrations in the 2050's are projected to increase by an average of +7 ppbv compared to the present-day. However, these results are spatially highly variable. Some regions may experience larger increases in average DM8H ozone, while other regions may experience decreases in average DM8H ozone. Projected changes in chemical boundary conditions are found to have the single largest impact on average DM8H ozone, and increase ozone levels in all regions. The second largest impact on ozone levels is due to changes in anthropogenic emissions combined with future land-use (i.e., reduced BVOC emissions), which increase ozone in most regions, except in large urban centers, where ozone decreases. Climate change alone is projected to increase average DM8H ozone in some regions (northeast and west central), and decrease it in others (west coast and south/southeast), but results in an overall decrease of ozone. When projected changes in climate and land-use are simultaneously accounted for, average DM8H ozone is decreased even further.

Projected increases in future A24-h PM$_{2.5}$ concentrations are primarily driven by increases in inorganic aerosol concentrations, which more than offset any decreases in biogenic SOA associated with the reduced BVOC emissions (from projected land-use changes). Projected changes in chemical boundary conditions result in a negligible increase (<1 μg m^{-3}) in A24-h PM$_{2.5}$ concentrations. Climate change tends to reduce PM$_{2.5}$ concentrations in most regions, with the largest reductions coming in the Southeastern US due to enhanced wet deposition from an increase in convective precipitation.

The results from this work show that although climate change may play an important role in defining future air quality in certain regions, on a larger scale, changes in chemical boundary conditions and emissions appear to play a much more important role. This is consistent with recent work by Tao et al. (2007) who show that the importance of specific global changes to projected air quality will change depending on which future climate/emissions scenario is assumed. Furthermore, the variability in the results from recent modeling studies examining the impact of global changes on US air quality (e.g. Wu et al., 2008; Racherla and Adams, 2008; Tagaris et al., 2007; Dentener et al., 2006; Murazaki and Hess, 2006) illustrates the difficulty involved in making these predictions, as well as the necessity for including all available studies when evaluating the potential impacts of global changes on future US air quality. The results presented here are representative of summertime climatology only, where the summertime is represented by five present-day or future July's. Although five July's are fairly representative of the middle of the ozone season, elevated $PM_{2.5}$ can occur year-round, and the climatological and emissions drivers that impact $PM_{2.5}$ in the summertime may be very different at other times of the year. To examine the relationship between specific global changes and regional air quality more thoroughly, we plan to conduct a matrix of additional model runs covering both summer and winter months, that will include multiple future climate, global/regional anthropogenic emissions, and land-use/land-cover scenarios.

Edited by: F. J. Dentener

References

Alcamo, J., Leemans, R., and Kreileman, E.: Global change scenarios of the 21st century. Results from the IMAGE 2.1 model. Pergamon & Elseviers Science, London, UK, 296 pp., 1998.

Binkowski F. S. and Roselle, S. J.: Models-3 Community Multiscale Air Quality (CMAQ) model aerosol component 1. Model description, J. Geophys. Res., 108(D6), 4183, doi:10.1029/2001JD001409, 2003.

Bonan, G. B., Oleson, K. W., Vertenstein, M., Levis, S., Zeng, X. B., Dai, Y. J., Dickinson, R. E., and Yang, Z. L.: The Land Surface Climatology of the Community Land Model Coupled to the NCAR Community Climate Model, J. Climate, 15(22), 3123–3149, 2002.

Byun, D. and Schere, K. L.: Review of the Governing Equations, Computational Algorithms, and Other Components of the Models-3 Community Multiscale Air Quality (CMAQ) Modeling System, Appl. Mech. Rev., 59, 51–77, 2006.

Carter, W.: Documentation of the SAPRC-99 Chemical Mechanism for VOC Reactivity Assessment, Draft report to the California Air Resources Board, Contracts 92–329 and 95–308, 8 May 2000a.

Carter, W.: Implementation of the SAPRC-99 Chemical Mechanism into the Models-3 Framework, Report to the United States Environmental Protection Agency, 29 January 2000b.

Chen, J., Avise, J., Lamb, B., Salathe, E., Mass, C., Guenther, A., Wiedinmyer, C., Lamarque, J.-F., O'Neill, S., McKenzie, D., and Larkin, N.: The effects of global changes upon regional ozone pollution in the United States, Atmos. Chem. Phys., submitted, 2008.

Civerolo, K. L., Sistla, G., Rao, S. T., and Nowak, D. J.: The Effects of Land Use in Meteorological Modeling: Implications for Assessment of Future Air Quality Scenarios, Atmos. Environ., 34(10), 1615–1621, 2000.

Constable, J., Guenther, A., Schimel, D., and Monson, R.: Modeling changes in VOC emission in response to climate change in the continental United States, Glob. Chang. Biol., 5, 791–806, 1999.

Dawson, J. P., Adams, P. J., and Pandis, S. N.: Sensitivity of ozone to summertime climate in the eastern USA: A modeling case study, Atmos. Environ., 41, 1494–1511, 2007.

Dentener, F., Stevenson, D., Ellingsen, K., et al.: The Global Atmospheric Environment for the Next Generation, Environ. Sci. Technol., 40, 3586–3594, 2006.

Eder, B. and Yu, S.: A performance evaluation of the 2004 release of Models-3 CMAQ, Atmos. Environ., 40, 4811–4824, 2006.

Grell, G. A., Dudhia, J., and Stauffer, D. R.: A Description of the Fifth-Generation Penn State/NCAR Mesoscale Model (MM5), National Center for Atmospheric Research, Boulder, CO, USA, NCAR/TN-398+STR, 122 pp., 1994.

Guenther, A., Karl, T., Harley, P., Wiedinmyer, C., Palmer, P. I., and Geron, C.: Estimates of global terrestrial isoprene emissions using MEGAN (Model of Emissions of Gases and Aerosols from Nature), Atmos. Chem. Phys., 6, 3181–3210, 2006, http://www.atmos-chem-phys.net/6/3181/2006/.

Heald, C. L., Henze, D. K., Horowitz, L. W., Feddema, J., Lamarque., J.-F., Guenther, A., Hess, P. G., Vitt, F., Seinfeld, J. H., Goldstein, A. H., Fung, I.: Predicted change in global secondary organic aerosol concentrations in response to future climate, emissions, and land use change, J. Geophys. Res., 113,

D05211, doi:10.1029/2007JD009092, 2008.

Hogrefe, C., Biswas, J., Lynn, B., Civerolo, K., Ku, J.-Y., Rosenthal, J. Rosenzweig, C., Goldberg, R., and Kinney, P. L.: Simulating regional-scale ozone climatology over the eastern United States: model evaluation results, Atmos. Environ., 38, 2627–2638, 2004a.

Hogrefe, C., Lynn, B., Civerolo, K., Ku, J.-Y., Rosenthal, J., Rosenzweit C., Goldberg R., Gaffin, S., Knowlton, K., and Kinney, P. L.: Simulating changes in regional air pollution over the eastern United States due to changes in global and regional climate and emissions, J. Geophys. Res., 109, D22301, doi:10.1029/2004JD004690, 2004b.

Horowitz, L. W.: Past, present, and future concentrations of tropospheric ozone and aerosols: Methodology, ozone evaluation, and sensitivity to aerosol wet removal, J. Geophys. Res., 111, D22211, doi:10.1029/2005JD006937, 2006.

Houyoux, M., Vukovich, J., and Brandmeyer, J. E.: Sparse Matrix Operator Kernel Emissions (SMOKE) modeling system user manual, University of North Carolina at Chapel Hill, online available at: http://www.smoke-model.org, last access: 2009, 2005.

Jaffe, D. A., Parish, D., Goldstein, A., Price, H., and Harris, J.: Increasing background ozone during spring on the west coast of North America, Geophys. Res. Lett., 30(12), 1613, doi:10.1029/2003GL017024, 2003.

Leung, L. R. and Gustafson Jr., W. I.: Potential regional climate and implications to US air quality, Geophys. Res. Lett., 32, L16711, doi:10.1029/2005GL022911, 2005.

Liao, K.-J., Tagaris, E., Manomaiphiboon, K., Wang, C., Woo, J.-H., Amar, P., He, S., and Russell, A. G.: Quantification of the impact of climate uncertainty on regional air quality, Atmos. Chem. Phys., 9, 865–878, 2009,
http://www.atmos-chem-phys.net/9/865/2009/.

Marenco, A., Gouget, H., Nédélec, P., Pagés, J.-P., and Karcher, F.: Evidence of a long term increase in tropospheric ozone from Pic du Midi data series: Consequences: positive radiative forcing, J. Geophys. Res., 99, 16617–16632, 1994.

Mickley, L. J., Jacob, D. J., and Field, B. D.: Effects of future climate change on regional air pollution episodes in the United States, Geophys. Res. Lett., 31, L24103, doi:10.1029/2004GL021216, 2004.

Murazaki, K. and Hess, P.: How does climate change contribute to surface ozone change over the United States?, J. Geophys Res., 111, D05301, doi:10.1029/2005JD005873, 2006.

Nakićenović, N., Alcamo, J., Davis, G., de Vries B., Fenhann, B., Gaffin, S., Gregory K., Grübler, A., Jung, T. Y., Kram, T., La Rovere, E. L., Michaelis, E. L., Mori, S., Morita, T., Pepper, W., Pitcher, H., Price, L., Raihi, K., Roehrl, A., Rogner, H.-H., Sankovski, A., Schlesinger, M., Shukla, P., Smith, S., Swart, R., van Rooijen, S., Victor, N., and Dadi, Z.: IPCC Special Report on Emissions Scenarios, Cambridge University Press, Cambridge, UK and New York, NY, USA, 2000.

Nenes, A., Pandis, S. N., and Pilinis, C.: ISORROPIA: A new thermodynamic equilibrium model for multiphase multicomponent inorganic aerosols, Aquat. Geochem., 4, 123–152, 1998.

Phillips, S. B. and Finkelstein, P. L.: Comparison of spatial patterns of pollutant distribution with CMAQ predictions, Atmos. Environ., 40, 4999–5009, 2006.

Racherla, P. N. and Adams, P. J.: The response of surface ozone to climate change over the Eastern United States, Atmos. Chem. Phys., 8, 871–885, 2008,
http://www.atmos-chem-phys.net/8/871/2008/.

RIVM (Rijks Instituut voor Volksgezondheid en Milieu): IMAGE 2.2 CD release and documentation. The IMAGE 2.2 implementation of the SRES scenarios: A comprehensive analysis of emissions, climate change and impacts in the 21st century, for further information online available at: http://www.rivm.nl/image/index.html, 2002.

Salathé, E. P., Steed, R., Mass, C. F., and Zahn, P.: A high-resolution climate model for the United States pacific northwest: Mesoscale feedbacks and local responses to climate change, J. Climate, in press, 2008.

Schell, B., Ackermann, I., Hass, H., Binkowski, F., and Ebel, A.: Modeling the formation of secondary organic aerosol within a comprehensive air quality model system, J. Geophys. Res., 106(D22), 28275–28293, 2001.

Sillman S. and Samson, P. J.: Impact of temperature on oxidant photochemistry in urban, polluted rural, and remote environments, J. Geophys. Res., 100, 11497-11508, 1995.

Staehelin, J., Thudium, J., Buehler, R., Volz-Thomas, A., and Graber, W.: Trends in Surface Ozone Concentrations at Arosa (Switzerland), Atmos. Environ., 28, 75–87, 1994.

Steiner, A. L., Tonse, S., Cohen, R. C., Goldstein, A. H., and Harley, R. A.: Influence of future climate and emissions on regional air quality in California, USA, J. Geophys. Res., 111, D18303, doi:10.1029/2005JD006935, 2006.

Stevenson, D. S., Johnson, C. E., Collins, W. J., Derwent, R. G., and Edwards, J. M.: Future estimates of tropospheric ozone radiative forcing and methane turnover - the impact of climate change, Geophys. Res. Lett., 105(14), 2073–2076, doi:10.1029/1999GL010887, 2000.

Strengers, B., Leemans, R., Eickhout, B., de Vries, B., and Bouwman, L.: The land-use projections and resulting emissions in the IPCC SRES scenarios as simulated by the IMAGE 2.2 model, GeoJournal, 61, 381–393, 2004.

Tagaris, E., Manomaiphiboon, K., Liao, K.-J., Leung, L. R., Woo, J.-H., He, S., Amar, P., and Russel, A. G.: Impacts of global climate change and emissions on regional ozone and fine particulate matter concentrations over the United States, J. Geophys. Res., 112, D14312, doi:10.1029/2006JD008262, 2007.

Tao, Z., Williams, A., Huang, H.-C., Caughey, M., and Liang, X.-Z.: Sensitivity of US surface ozone to future emissions and climate changes, Geophys. Res. Lett., 34, L08811, doi:10.1029/2007GL029455, 2007.

Theobald, D. M.: Landscape Patterns of Exurban Growth in the USA From 1980 to 2020, Ecol. Soc., 10(1), p. 32, 2005.

US EPA: Economic Growth Analysis System (EGAS) version 5.0 User Manual, US Environmental Protection Agency, 2004.

van Aardenne, J. A., Carmichael, G. R., Levy II, H., Streets, D., and Hordijk, L.: Anthropogenic NOx emissions in Asia in the period 1990-2020. Atmos. Environ., 33, 633–646, 1999.

Varotsos, C. and Cartalis, C.: Re-evaluation of surface ozone over Athens, Greece, for the period 1901–1940, Atmos. Res., 26, 303–310, 1991.

Vingarzan, R. and Thomson, B.: Temporal variation in daily concentrations of ozone and acid related substances at Saturna Island, British Columbia, J. Air Waste Manage. Assoc., 54, 459–472, 2004.

Washington, W. M., Weatherly, J. W., Meehl, G. A., Semtner, A. J., Bettge, T. W., Craig, A. P., Strand, W. G., Arblaster, J., Wayland, V. B., James, R., and Zhang, Y.: Parallel Climate Model (PCM) control and transient simulations. Climate Dyn., 16(10–11), 755–774, 2000.

Wiedinmyer, C., Tie, X., Guenther, A., Neilson, R., and Granier, C.: Future changes in biogenic isoprene emissions: how might they affect regional and global atmospheric chemistry?, Earth Int., 10(3), 1–19, 2006.

Wu, S., Mickley, L. J., Leibensperger, E. M., Jacob, D. J., Rind, D., and Streets, D. G.: Effects of 2000–2050 global change on ozone air quality in the United States, J. Geophys. Res., 113, D06302, doi:10.1029/2007JD008917, 2008.